

Northeastern University

Electrical and Computer Engineering Faculty Publications

Department of Electrical and Computer Engineering

May 01, 1990

Continuous steering of MSSW waves in YIG double-layers

K. Q. Sun

C. Vittoria
Northeastern University

Recommended Citation

Sun, K. Q. and Vittoria, C., "Continuous steering of MSSW waves in YIG double-layers" (1990). *Electrical and Computer Engineering Faculty Publications*. Paper 29. http://hdl.handle.net/2047/d20002199

This work is available open access, hosted by Northeastern University.



Continuous steering of MSSW waves in YIG double layers

Kunquan Sun and Carmine Vittoria

Citation: J. Appl. Phys. 67, 5495 (1990); doi: 10.1063/1.345862

View online: http://dx.doi.org/10.1063/1.345862

View Table of Contents: http://jap.aip.org/resource/1/JAPIAU/v67/i9

Published by the American Institute of Physics.

Related Articles

Frequency multiplying behavior in a magnetoelectric unimorph Appl. Phys. Lett. 100, 032903 (2012)

Magnetoelectric nonlinearity in magnetoelectric laminate sensors

J. Appl. Phys. 110, 114510 (2011)

Single-layer magnetic memory based on Rashba three-terminal quantum dot device

J. Appl. Phys. 110, 093713 (2011)

Effects of hysteresis losses on dynamic behavior of magnetostrictive actuators

J. Appl. Phys. 110, 093908 (2011)

Hybrid spintronics and straintronics: A magnetic technology for ultra low energy computing and signal processing Appl. Phys. Lett. 99, 063108 (2011)

Additional information on J. Appl. Phys.

Journal Homepage: http://jap.aip.org/

Journal Information: http://jap.aip.org/about/about_the_journal Top downloads: http://jap.aip.org/features/most_downloaded

Information for Authors: http://jap.aip.org/authors

ADVERTISEMENT



Continuous steering of MSSW waves in YIG double layers

Kunguan Sun and Carmine Vittoria

Department of Electrical and Computer Engineering, Northeastern University, Boston, Massachusetts 02115

In this paper we report on the calculations for the magnetostatic wave propagation characteristics in single-crystal double layers of yttrium iron garnet with arbitrary direction of magnetization. The induced uniaxial magnetic anisotropy field is assumed to be different in the two layers, and hence the magnetization in one layer is aligned at an angle with respect to the magnetization direction in the other layer. The magnetostatic surface wave propagations with the greatest bandwidths and the maximum energy deliveries in each layer can be strongly affected by the application of an applied magnetic field and the magnetostatic coupling between the two layers.

Since Wolfram¹ first described magnetostatic waves in double-layered magnetic layers, several investigators²⁻¹¹ have studied layered systems. In all the studies, 1-11 it has been assumed that the magnetizations of each individual layer in double-layered structures are either parallel or antiparallel. In this paper we consider the effect of noncollinear magnetization direction on magnetostatic wave propagation in a two-layered magnetic system. We assume that the magnetization in a given magnetic layer to be aligned in an arbitrary direction with respect to the magnetization direction in the other layer of a doublelayered structure. It has recently been determined experimentally¹² that when the applied magnetic field is small the magnetizations in each layer of a single-crystal double-layer YIG structure are not parallel to each other due to the induced in-plane anisotropy field H_u being different in each layer. H_u is found 12 to be different in each layer, since the strain due to the substrate strain is different in each layer.

Specifically, the present work aims to study the propagation characteristics of magnetostatic surface wave (MSSW) in a single-crystal structure of GGG/YIG/GGG/YIG, where GGG is the abbreviation for gadolinium gallium garnet. The magnetization orientations in the two YIG films are not collinear when the applied field is small. General formulation of the dispersion relations is derived for both YIG films with cubic and induced in-plane anisotropy fields in Sec. II. Calculated results for the dispersion relations as a function of magnetic field and separation of the two YIG layers and potential applications are illustrated in Sec. III. In Sec. IV. conclusions are drawn.

The geometry of the two-layered structure and angular orientations of \mathbf{M}_1 and \mathbf{M}_2 are shown in Fig. 1, where a paramagnetic GGG film of thickness d_2 is placed between two YIG films, the GGG substrate (d_4) is assumed to be infinitely thick, and the capital letters, X_c , Y_c , and Z_c refer to the crystal axes, while (ϕ,β) , (ϕ_1,θ_1) , and (ϕ_2,θ_2) refer to the angular distributions of \mathbf{H}_a , \mathbf{M}_1 , and \mathbf{M}_2 , respectively. The two YIG films were grown epitaxially so that their planes are crystallographically equivalent. Two coordinate systems are introduced, since there are two magnetic layers to consider. The primed system (x',y',z') corresponds to layer 1 (\mathbf{M}_1) and the unprimed (x,y,z) to layer 2 (\mathbf{M}_2) . We

choose z' and z to be parallel to the static magnetization direction M_1 and M_2 , respectively; see Fig. 1.

An external static magnetic field H_a is applied in the film plane so that the internal fields $\mathbf{H}_0^{(1)}$ and $\mathbf{H}_0^{(2)}$ also lie in the planes of the two YIG layers. The quantities $H_0^{(1)}$ and $\mathbf{H}_0^{(2)}$ can be expressed ¹³ in terms of the external field \mathbf{H}_a , the static cubic anisotropy field components $H_A^{(1)}$ and $H_A^{(2)}$, and the static-induced in-plane anisotropy field components $\mathbf{H}_{u}^{(1)}$ and $\mathbf{H}_{u}^{(2)}$, where the superscripts (1) and (2) denote the layers corresponding to M_1 and M_2 . Mathematical expressions for $H_0^{(1)}$ and $\mathbf{H}_0^{(2)}$ are given as 14 $\mathbf{H}_0^{(i)} = \mathbf{H}_a + \mathbf{H}_A^{(i)} + \mathbf{H}_u^{(i)}$, i = 1,2. As in previous theoretical developments, ¹³ the magnetostatic dispersion relations may be expressed in terms of permeability tensor elements for each magnetic layer. We start with the well-known Landau-Lifshitz equation of motion with no damping and adapt previous formulations 13 for the case of the applied field in the (110) plane. After some algebraic manipulations, the permeability tensors corresponding to H_a applied in the film plane (i = 1,2) are obtained where $\mu_{11}^{(i)} = 1 - \Omega_{\nu} / (\Omega_i^2)$

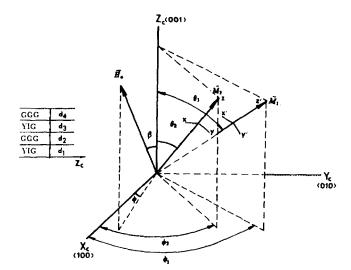


FIG. 1. A crossview of the geometrical configuration of the double-layered YIG film and three coordinate systems of interest. The capital letters X_c , Y_c , and Z_c refer to the crystal axes. (x_c, y, z) and (x', y', z') refer to layer 2 (\mathbf{M}_2) and layer 1 (\mathbf{M}_1) ; z and z' are parallel to \mathbf{M}_2 and \mathbf{M}_1 , respectively.

5495 J. Appl. Phys. 67 (9), 1 May 1990

0021-8979/90/095495-03\$03.00

© 1990 American Institute of Physics

5495

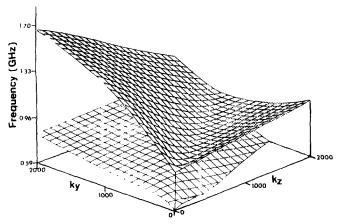


FIG. 2. Three-dimensional dispersion (ω, k_y, k_z) . H = 0, $\alpha = 24^\circ$, and $d_y = 1 \mu m$.

 $\mu_{22}^{(i)} = 1 - \Omega_{x_i} / (\Omega_i^2 - \Omega_{y_i}^2),$
$$\begin{split} &-\Omega H_{i}^{2}, \quad \Omega_{x_{i}} = (H_{0}^{(i)} - M_{i}a_{i})/4\pi M_{i}, \quad \Omega_{y_{i}} = (H_{0}^{(i)} - M_{i}b_{i})/4\pi M_{i}, \quad \Omega_{y_{i}} = (H_{0}^{(i)} - M_{i}b_{i})/4\pi M_{i}, \quad \Omega_{i} = (\omega/|\gamma|)(1/4\pi M_{i}), \\ &\Omega H_{i}^{2} = \Omega_{x_{i}}\Omega_{y_{i}}, a_{i} = 2K_{1}^{(i)}(1.5\sin^{2}\theta_{i} - 1)/M_{i}^{2}, \\ &b_{i} = 2K_{1}^{(i)}(1.125\sin^{2}\theta_{i} - 1)/M_{i}^{2} - 2K_{u}^{(i)}\sin\theta_{i}/M_{i}^{2}, \text{ and} \end{split}$$
i = 1,2 denote the coordinate systems (x',y',z') and (x,y,z)associated with the magnetizations M_1 and M_2 , respectively. $K_1^{(i)}$ and $K_{\mu}^{(i)}$ are the cubic magnetocrystalline and the uniaxial anisotropy energy constants, respectively. The coefficients a_i and b_i have been derived previously. 12 By solving the equilibrium condition equations based on minimizing the free energy of each magnetic layer, it is found 14 that the equilibrium azimuthal angles of M₁ and M₂ are equal to 45°, or $\phi_1 = \phi_2 = 45^\circ$, since \mathbf{H}_a is in the film plane. This implies that both M_1 and M_2 lie in the $\{1\overline{1}0\}$ plane, which is also the film plane. The polar angles θ_1 and θ_2 are the equilibrium angles for M_1 and M_2 with respect to the Z_c axis, and they are not equal if the applied magnetic field is low compared to the magnetic anisotropy fields $H_u^{(1)}$ and $H_u^{(2)}$. Both y' and y

lie in the film plane, but x' and x are directed normal to the film plane. The angle between y' and y or z' is equal to $\theta_1 - \theta_2 = \alpha$ and is a measure of misalignment between the two magnetization directions. We will examine the magnetostatic wave propagation in (x,y,z) system as shown in Fig. 1. The angular parameters (ϕ_1,θ_1) and (ϕ_2,θ_2) at equilibrium are substituted into Eq. (2) in order to determine the permeabilities $\mu^{(1)}$ and $\mu^{(2)}$.

Under the magnetostatic approximation $\mathbf{h}_m = -\nabla \psi$, where ψ is a magnetic scalar potential, combined with $\mathbf{B} = \mu_0 \mu \cdot \mathbf{h}_m$, we can have five Laplace equations and corresponding solutions for five regions. By using the boundary conditions, that the tangential components of \mathbf{h}_m and normal components of \mathbf{B} are continuous, the following transcendental equation is obtained:

$$(P^{(1)}Q^{(1)}e^{-2\kappa'd_1} - 1)(1 - P^{(2)}Q^{(2)}e^{-2\kappa d_1}) + P^{(1)}Q^{(2)}e^{-2\kappa d_2}(1 - e^{-2\kappa d_1})(1 - e^{-2\kappa'd_1}) = 0, (1)$$

where

$$\begin{split} P^{(1)} &= \frac{1 - p^{(1)}}{1 + p^{(1)}}, \quad P^{(2)} &= \frac{1 - p^{(2)}}{1 + p^{(2)}}, \\ Q^{(1)} &= \frac{1 - q^{(1)}}{1 + q^{(1)}}, \quad Q^{(2)} &= \frac{1 - q^{(2)}}{1 + q^{(2)}}, \\ p^{(1)} &= \frac{\kappa'}{k} \mu_{11}^{(1)} + \left(\frac{k_y}{k} \cos \alpha - \frac{k_z}{k} \sin \alpha\right) \mu_{12}^{(1)}, \\ p^{(2)} &= \frac{\kappa}{k} \mu_{11} + \frac{k_y}{k} \mu_{12}, \\ q^{(1)} &= \frac{\kappa'}{k} \mu_{11}^{(1)} - \left(\frac{k_y}{k} \cos \alpha - \frac{k_z}{k} \sin \alpha\right) \mu_{12}^{(1)}, \\ q^{(2)} &= \frac{\kappa}{k} \mu_{11} - \frac{k_y}{k} \mu_{12}, \end{split}$$

and (κ, k_y, k_z) and κ', k_y', k_z') are the wave numbers corresponding to (x,y,z) and (x',y',z') coordinate systems, respectively, and $k^2 = k_y^2 + k_z^2$

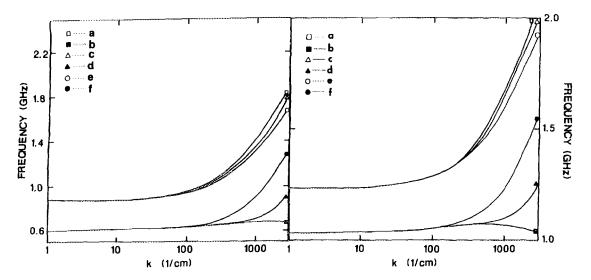


FIG. 1. A crossview of the geometrical configuration of the double-layered YIG film and three coordinate systems of interest. The capital letters X_c , Y_c , and Z_c refer to the crystal axes. (x,y,z) and (x',y',z') refer to layer 2 (\mathbf{M}_2) and layer 1 (\mathbf{M}_1) ; z and z' are parallel to \mathbf{M}_2 and \mathbf{M}_3 , respectively.

J. Appl. Phys., Vol. 67, No. 9, 1 May 1990

5496

K. Sun and C. Vittoria

5496

$$\kappa^{2} = \frac{\mu_{22}}{\mu_{11}} k_{y}^{2} + \frac{1}{\mu_{11}} k_{2}^{2}, \quad (\mu_{11} = \mu_{11}^{(2)}, \ \mu_{22} = \mu_{22}^{(2)}),$$

$$\kappa'^{2} = \frac{\mu_{21}^{(1)}}{\mu_{11}^{(1)}} (k_{y}^{2} \cos^{2} \alpha - k_{y} k_{z} \sin 2\alpha + k_{z}^{2} \sin^{2} \alpha)$$

$$+ \frac{1}{\mu_{11}^{(1)}} (k_{y}^{2} \sin^{2} \alpha + k_{y} k_{z} \sin 2\alpha + k_{z}^{2} \cos^{2} \alpha).$$

Equation (2) includes two terms: The first term is recognized as the dispersion of two individual magnetic layers which are not magnetically and electromagnetically coupled, and the second term includes the effect of the coupling between the two magnetic layers.Limiting cases to consider are (1) $M_1 = M_2$; Eq. (2) results in a single dispersion relation which is consistent with that given in Ref. 8; (2) in the limit of either $d_2 = \infty$ or 0, $\mathbf{M}_1 = \mathbf{M}_2$; Eq. (2) reduces to the dispersion equation for a single layer derived by Damon and Eshbach. 15

Now we examine the general case in which d_1 , d_2 , and d_3 are finite. Here we are only interested in the magnetostatic wave propagations perpendicular to the static magnetizations, since they have the greatest bandwidths¹⁵ and the maximum energy deliveries. ¹⁴ If M_1 is parallel to M_2 , it is easy to demonstrate Eq. (2) in a two-dimensional dispersion (ω vs $|\mathbf{k}|$), where \mathbf{k} is perpendicular to either magnetizations. For M_1 not parallel to M_2 ($\alpha \neq 0$), our case of interest, the magnetostatic waves with the greatest bandwidths and maximum energy delivery propagate in the directions contained in the y-z plane, and we would expect the angle between the MSSW propagations with the described properties in the two films to be α , if d_2 is very large. This is due to the fact that the angle between M_1 and M_2 is α and the interested MSSW propagations are normal to M_1 and M_2 , respectively. As d_2 is reduced, the magnetostatic coupling between films is increased. The effect of the coupling is to change the group velocities of magnetostatic waves in the whole y-z plane. In some region of the $\omega(k_y,k_z)$ plot, there exists dispersion for negative group velocities. In order to clearly view propagation properties of magnetostatic waves in the y-z plane, it is meaningful to plot dispersions in three dimensions (ω vs k_y and k_z , for example). In either the strong or weak coupling regime, the MSSW wave with the greatest bandwidth and the maximum energy delivery is still focused perpendicular to the static magnetization in each layer.

Based on the dispersion equation (2), a three-dimensional plot (ω vs k_{ν} and k_{z}) is obtained (see Fig. 2), where two MSSW branches are exhibited. The assumed parameters for one layer are $4\pi M = 1750$ G, $2K_1/M_s = -82$ Oe, $2K_{\mu}/M_s = 0$, and $d_1 = 1 \mu m$; for the other layer, $4\pi M = 1256$ G, $2K_1/M_s = -82$ Oe, $2K_u/M_s = 50$ Oe, and $d_3 = 1 \mu m$. The separation between the two magnetic layers is $d_2 = 1 \mu m$, and the applied field $H_a = 0.4 \pi M$ implies in our case $4\pi M_{\rm eff}$, where $4\pi M_{\rm eff} = 4\pi M_s + 2K_s/M_s$. K_s is the uniaxial magnetic anisotropy energy parameter whose uniaxial axis is normal to the film plane. This is to contrast to H_u in which the uniaxial axis is in the plane. The top branch corresponds to layer 1, while the bottom branch corresponds to layer 2. Due to the different static magnetiz-

ations and induced in-plane anisotropy fields H_u in the two different layers and the coupling between the two layers, the dispersion for layer 1 differs from that of layer 2. One feature of the bottom branch is that there exists a cutoff frequency region. The other feature is the existence of an anomalous region where $d\omega/dk < 0.2.5$

Since the MSSW propagations perpendicular to the static magnetizations have the greatest bandwidths and the maximum energy deliveries, we are only interested in propagations normal to the static magnetizations. This is implied in the following calculations. From the parameters used in Fig. 2, the angle between the two static magnetizations was determined as 24°. This implies that the interesting wave propagations in the two layers are 24° away. Two branches of the dispersion corresponding to the interesting MSSW waves in the two layers are shown in Fig. 3(a) (see curves cand d). While the separation between the two layers changes with other parameters being the same, the angle between the two interesting propagations is not affected. However, the splitting between the two branches of the dispersion changes. The smaller the separation, the bigger the splitting between the two branches. The effect of the separation on the dispersion can be shown in Fig. 3(a), where curves a and b, cand d, and e and f correspond to the separations 0.1, 1, and $10 \,\mu\text{m}$, respectively. When a dc field of 50 G is applied to the two layer system along the (111) direction, the angle between M_1 and M_2 decreases to 13°. Therefore, MSSW propagations with the greatest bandwidths and the maximum energy deliveries are divergent by 13°, and the corresponding dispersions are shown in Fig. 3(b), where the separations 0.1, 1, and 10 μ m were used in the calculation. Further increasing the bias magnetic field aligns M₁ and M₂ together and MSSW waves with the desired properties in both layers propagate along the same direction. It is found from Figs. 3(a) and 3(b) that the bias magnetic field can steer the interested propagations in the two different layers and also change the operating frequency range.

The authors wish to thank ONR for supporting the research in part. Also, we want to thank Dr. P. De Gasperis, Dr. R. Marcelli, and Dr. H. L. Glass for useful discussions pertaining to this work.

```
<sup>1</sup>T. Wolfram, J. Appl. Phys. 41, 4748 (1970).
```

5497

² A. K. Ganguly and C. Vittoria, J. Appl. Phys. 45, 4665 91974).

³ L. R. Adkins and H. L. Glass, J. Appl. Phys. 53, 8928 (1982).

M. R. Daniel and P. R. Emtage, J. Appl. Phys. 53, 3723 (1982) ⁵ V. I. Zubkov and V. A. Epanechnikov, Sov. Tech. Phys. Lett. 11, 585

⁶H. Pfeiffer, Phys. Status Solidi A 18, K53 (1973).

⁷ N. S. Chang and Y. Matsuo, Proc. IEEE 66, 1577 (1978).

⁸ H. Sasaki and N. Mikoshiba, J. Appl. Phys. 52, 3546 (1981).

⁹ P. Grünberg, J. Appl. Phys. **52**, 6824 (1980). ¹⁰ J. P. Perekh and K. W. Chang, IEEE Trans. Magn. MAG-18, 1610

¹¹ R. E. Camley, R. S. Rahman, and D. L. Mills, Phys. Rev. B 27, 261 (1983).

¹² K. Sun and C. Vittoria (unpublished).

¹³C. Vittoria and N. D. Wilsey, J. Appl. Phys. 45, 414 (1974).

¹⁴ K. Sun and C. Vittoria (unpublished).

¹⁵ R. W. Damon and J. R. Eshbach, J. Phys. Chem. Solids 19, 308 (1961).